A general analytical solution for groundwater fluctuations due to dual tide in long but narrow islands

Ching-Sheng Huang,[1] Hund-Der Yeh,[1] and Chia-Hao Chang[1]

Received 28 July 2011; revised 14 February 2012; accepted 26 March 2012; published 4 May 2012.

[1] This paper develops a general mathematical model for describing head fluctuations in an aquifer of long but narrow islands subject to a dual tide effect. The upper boundary condition of the aquifer is represented by an equation combining the simplified free surface equation with a leakage term. Such an equation is considered as a general expression representing the upper boundary condition of a confined, unconfined, or leaky confined aquifer. The closed-form solution of the model represented by two series terms is developed by the direct Fourier method and finite Fourier sine transform. One of the series can reduce to a closed-form expression by means of contour integral and residue theorem. If the width of the island is very large, this solution gives the predicted head almost the same as that of the solution for an aquifer subject to a single tide effect. It is found that the presence of an upper aquitard produces significant vertical flow in the lower leaky confined aquifer even if the aquitard permeability is low. Neglecting such vertical flow may result in an overestimate of hydraulic head in the leaky confined aquifer. The attenuation factor and phase lag predicted from the present solution subject to the dual tide effect agree well with those estimated from 57 day head fluctuation data observed at Garden Island, Australia.

Citation: Huang, C.-S., H.-D. Yeh, and C.-H. Chang (2012), A general analytical solution for groundwater fluctuations due to dual tide in long but narrow islands, *Water Resour. Res.*, *48*, W05508, doi:10.1029/2011WR011211.

1. Introduction

[2] There are some long but narrow islands in the world. Examples include Long Island located southeast of New York, U. S., Lido Island and Pellestrina Island in northern Italy, and Macquarie Island in the Southern Ocean lying southeast of Tasmania. The groundwater of those islands may fluctuate due to a tidal effect from both sides of the islands. Fire Island is also an example. This island is located at the south shore of Long Island and is 49 km long and 225–750 m in width. The island aquifer consists of gravel and fine to coarse sand, and its hydraulic conductivity is about 60 m day^{-1} [*Bokuniewicz and Pavlik*, 1990]. Under such geometry and formation, the groundwater in Fire Island is very likely to be influenced by both sides of the tide. Another example is Maui Island in the islands of Hawaii. The narrowest width occurring near the center of Maui Island is about 11 km. The Maui aquifer is generally composed of Wailuku Basalt in the west as well as Honomanu Basalt and Kula Volcanics in the east. The hydraulic conductivity ranges from 1 to 2500 m day^{-1} [*Rotzoll et al.*, 2007]. According to *Rotzoll et al.*'s [2008] report, groundwater in the center of Maui Island has been affected by the tides from both sides. Garden Island in Australia is the other example. Its geological formation and hydrological information are described in detail in section 3.5. The mathematical model for describing groundwater fluctuations subject to a single tide effect is obviously not suitable to be applied to these three islands mentioned above. Accordingly, there may be a need to develop a model for a dual tide in the groundwater systems of long but narrow islands.

[3] A number of analytical solutions had been developed for describing head fluctuations in a groundwater flow system subject to a single tide effect. Those solutions are categorized into three different sorts of aquifers: a confined aquifer [e.g., *Li and Chen*, 1991; *Geng et al.*, 2009], a leaky confined aquifer [e.g., *Li and Jiao*, 2001; *Guo et al.*, 2007; *Li et al.*, 2008], and an unconfined aquifer [e.g., *Teo et al.*, 2006; *Kacimov and Adballa*, 2010; *Balugani and Antonellini*, 2011].

[4] *Ferris* [1951] presented an analytical solution to describe groundwater fluctuations due to a single tide effect in a confined aquifer and used the solution as a basis to estimate the aquifer transmissibility. *Guo et al.* [2010] developed an analytical solution for a confined aquifer consisting of two zones with different hydraulic parameters. Some articles are involved in the development of analytical solutions for a confined aquifer extending infinitely or finitely under the sea. *Van Der Kamp* [1972] developed an analytical solution for a confined aquifer extending infinitely under the sea. *Li et al.* [2007] presented an analytical solution for a confined aquifer extending finitely with a semipermeable outlet cap. These two solutions considered a term for tidal loading in the governing equation.

[5] *Chen and Jiao* [1999] mentioned that coastal aquifer systems usually consist of one overlying unconfined aquifer, one underlying leaky confined aquifer, and an aquitard between them. The water table of the overlying unconfined

[1]Institute of Environmental Engineering, National Chiao Tung University, Hsinchu, Taiwan.

0043-1397/12/2011WR011211

aquifer is usually not influenced by the tide because of its aquifer storage [*Millham and Howes*, 1995] and thus treated as static. Therefore, most of analytical solutions dealing with the groundwater fluctuations in the leaky confined aquifer neglect the tidal effect on the water table of the overlying unconfined aquifer. Those solutions used one-dimensional (1-D) transient groundwater flow equation to describe the flow and treated the leakage through the aquitard as a sink term in the governing equation; that is, the vertical flow induced from the leakage is neglected. For example, *Jiao and Tang* [1999] developed an analytical solution for describing groundwater fluctuations in such a tidal leaky confined aquifer. *Chuang et al.* [2010] further derived an analytical solution for a heterogeneous tidal leaky confined aquifer. The aquifer is divided into several zones with different parameters, and thus their solution is expressed in a matrix form. *Xia et al.* [2007] developed an analytical solution for the leaky confined aquifer extending finitely under the sea and covered with a semipermeable outlet cap. Some articles proposing an analytical solution for the underlying leaky confined aquifer considered the tidal effect on the water table in the overlying unconfined aquifer. For example, *Jeng et al.* [2002] considered such an effect for a leaky confined aquifer. *Chuang and Yeh* [2007] also considered the effect for a leaky confined aquifer extending infinitely under the sea. Under the effect, *Chuang and Yeh* [2008] considered a leaky confined aquifer extending finite distance under the sea and covered with a permeable outlet cap. *Chuang and Yeh* [2011] further considered the same aquifer but a semipermeable outlet cap. These four articles presented an analytical solution to describe groundwater fluctuations in the upper unconfined and lower leaky confined aquifers.

[6] Analytical solutions for tidal unconfined aquifers may be categorized according to whether the mathematical model is linear or nonlinear. The nonlinear mathematical model includes a moving tidal boundary due to a sloping beach, nonlinear governing equation such as Boussinesq equation, or nonlinear free surface equation with second-order terms. On the other hand, the linear mathematical model excludes any one of these three nonlinear effects. The linear model generally has a vertical beach, linear governing equation to the unknown hydraulic head, and simplified free surface equation with neglecting the second-order terms. The perturbation technique was very commonly used to solve the nonlinear model. The solutions derived by this technique are expanded by a perturbation factor in a few series terms with small orders. The solutions generally give good results if the perturbation factor is small. Note that there is a problem of overhight in unconfined aquifers due to nonlinear effects arisen from the sloping beach, nonlinear free surface, and/or nonlinear governing equation. *Li et al.* [2000] used a 1-D linearized Boussinesq equation by considering the effect of the sloping beach to develop a first-order analytical solution for an unconfined aquifer. *Song et al.* [2007] used a 1-D nonlinear Boussinesq equation by considering a vertical beach to derive a second-order analytical solution for an unconfined aquifer. Other researches use two-dimensional (2-D) linear transient groundwater flow equation with a nonlinear free surface equation for an unconfined aquifer. The solution is available only for the water table and not for the whole flow domain. *Teo et al.* [2003] used a perturbation technique to derive an analytical solution for describing water table fluctuations in an unconfined aquifer with a sloping beach. Their solution gives good result when the aquifer thickness is rather thin (i.e., small perturbation factor). Some researchers developed a linear model for an unconfined aquifer. The solution derived from such a model has no restriction on the small perturbation factor. *Yeh et al.* [2010] used a 2-D linear transient groundwater flow equation to develop an analytical solution for describing groundwater fluctuations in an unconfined aquifer with a vertical beach. Their head solution is applicable to the whole flow domain.

[7] There are few articles devoted to the development of nonlinear mathematical models for coastal aquifer systems. For example, *Chuang et al.* [2012] used a 1-D nonlinear governing equation for the overlying unconfined aquifer and a 1-D linear governing equation for the underlying leaky confined aquifer. These two equations are coupled by a sink term of leakage through the aquitard. Based on perturbation technique, they presented a second-order analytical solution for both aquifers.

[8] Some studies dealt with the problems of island aquifers subject to the effect of a dual tide. *Rotzoll et al.* [2008] used 1-D linear transient groundwater flow equation to approximate unconfined aquifers based on Dupuit assumption. They developed an analytical solution for describing groundwater fluctuations under a dual tide effect. They reported that the groundwater fluctuations predicted from their solution for the island of Maui, Hawaii gave very good match with the observed data taken there. *Sun et al.* [2008] presented an analytical solution for head fluctuations in an island leaky confined aquifer. The leakage through an aquitard is also treated as a sink term in the governing equation. *Chang et al.* [2010] derived an analytical solution based on perturbation technique to describe water table fluctuations due to a dual tide in a shallow unconfined aquifer with two sloping beaches. Yet, the solution of head fluctuations they derived is only applicable to water table.

[9] Those articles discussed above are summarized in Table 1 for confined and leaky confined aquifers and in Table 2 for unconfined aquifers. The solutions listed in Table 1 are categorized based on the type of aquifer and tidal boundary, while those in Table 2 are according to the governing equation, nonlinear effect, and tidal boundary.

[10] This paper aims at developing a 2-D mathematical model for describing the behaviors of groundwater flow due to the effect of a dual tide in island aquifers. The top boundary condition of the aquifer is represented by the first-order free surface equation coupled with a leakage term. A closed-form solution of the model is derived by direct Fourier method, finite Fourier sine transform, and contour integral. This solution can be applied to predict the head fluctuations due to the effect of a dual tide in a confined, unconfined, or leaky confined aquifer and also the case of an island with a large width under a single tide effect. Additionally, the solution can also be used to identify the hydraulic parameters if coupled with an optimization approach in aquifer data analyses. The effect of specific yield on the amplitude and phase lag of groundwater fluctuations is investigated based on the developed solution for an unconfined aquifer. The effects of both the

Table 1. Classification of Previous Analytical Solutions for Various Confined and Leaky Confined Aquifers

Type of Aquifer	Tidal Boundary	References
1-D Groundwater Flow Equation		
Confined aquifer	Single tide	*Ferris* [1951]
Island confined aquifer	Dual tide	*Rotzoll et al.* [2008]
Confined aquifer divided into two zones with different hydraulic parameters	Single tide	*Guo et al.* [2010]
1-D Groundwater Flow Equation With Source Term of Tidal Loading		
Confined aquifer extending infinitely under the sea	Single tide	*Van Der Kamp* [1972]
Confined aquifer[a]	Single tide	*Li et al.* [2007]
1-D Groundwater Flow Equation With Sink Term of Aquitard Leakage		
Leaky confined aquifer[b]	Single tide	*Jiao and Tang* [1999]
Leaky confined aquifer[c]	Single tide	*Jeng et al.* [2002]
Heterogeneous leaky confined aquifer[b]	Single tide	*Chuang et al.* [2010]
Island leaky confined aquifer[b]	Dual tide	*Sun et al.* [2008]
1-D Groundwater Flow Equation With Sink Term of Aquitard Leakage and Source Term of Tidal Loading		
Leaky confined aquifer[a,b]	Single tide	*Xia et al.* [2007]
Leaky confined aquifer extending infinitely under the sea[c]	Single tide	*Chuang and Yeh* [2007]
Leaky confined aquifer[c,d]	Single tide	*Chuang and Yeh* [2008]
Leaky confined aquifer[a,c]	Single tide	*Chuang and Yeh* [2011]

[a,d]Aquifer extends finitely under the sea with [a]semipermeable or [d]permeable outlet cap.
[b,c]Tide effect on overlying unconfined aquifer is [b]neglected or [c]considered.

vertical hydraulic conductivity in unconfined aquifers and the leakage in leaky confined aquifers on the vertical flow are also examined. In addition, the attenuation factor and phase lag estimated by the present solution are compared with those estimated from observed data taken at Garden Island, Australia reported by *Trefry and Bekele* [2004].

2. Method

2.1. Mathematical Model

[11] A mathematical model is developed for describing the head fluctuation in the tidal aquifer system which can be a confined aquifer, an unconfined aquifer, or a leaky confined aquifer consisting of an upper unconfined aquifer, a lower confined aquifer, and an aquitard in between. Figure 1 illustrates the conceptual model for a 2-D leaky confined aquifer system in a long but narrow island. The origin of Cartesian coordinate system is located at the intersection of the vertical beach and mean sea level (MSL). The MSL is chosen as reference datum where the potential head is zero. The width of the aquifer system is denoted as l. The thickness of the leaky confined aquifer is b, and the thickness of the aquitard is b'. The tide amplitudes on the left-hand side (LHS) and right-hand side (RHS) of the aquifer are A_1 and A_2, respectively.

[12] Consider that the aquifer is homogeneous and anisotropic, and the difference in density between seawater and groundwater is neglected. The governing equation for describing the head fluctuation $h(x,z,t)$ is therefore expressed as [*Teo et al.*, 2003]

$$K_x \frac{\partial^2 h}{\partial x^2} + K_z \frac{\partial^2 h}{\partial z^2} = S_s \frac{\partial h}{\partial t}, \tag{1}$$

where K_x and K_z are horizontal and vertical hydraulic conductivities, respectively, and S_s is specific storage. The bottom boundary condition representing the impermeable layer is

$$\frac{\partial h}{\partial z} = 0 \quad \text{at} \quad z = -b. \tag{2}$$

[13] The tide is considered to perfectly connect with the groundwater because the coastal aquifer usually consists of sandy materials. Thus, the boundary conditions on the LHS and RHS of the aquifer are, respectively, denoted as

$$h = A_1 \cos(w_1 t) \quad \text{at} \quad x = 0 \tag{3}$$

and

$$h = A_2 \cos(w_2 t + \phi) \quad \text{at} \quad x = l, \tag{4}$$

where w_1 and w_2 are tidal frequencies and ϕ is the phase difference between the LHS and RHS tidal boundaries.

[14] The leakage through the aquitard happens on the top of the leaky confined aquifer, and the water table in upper

Table 2. Classification of Previous Analytical Solutions for Unconfined Aquifers

Governing Equation	Nonlinear Effects	Tidal Boundary	References
1-D linearized Boussinesq equation	Sloping beach	Single tide	*Li et al.* [2000][a]
1-D Boussinesq equation	With a second-order term $h\,\partial h/\partial x$ in governing equation	Single tide	*Song et al.* [2007][a]
2-D groundwater flow equation	Sloping beach and second-order free surface equation	Single tide	*Teo et al.* [2003][a]
2-D groundwater flow equation	Sloping beach and second-order free surface equation	Dual tide	*Chang et al.* [2010][a]
2-D groundwater flow equation	None	Single tide	*Yeh et al.* [2010][b]

[a]Solution derived by using perturbation technique.
[b]Solution derived by using integral transforms.

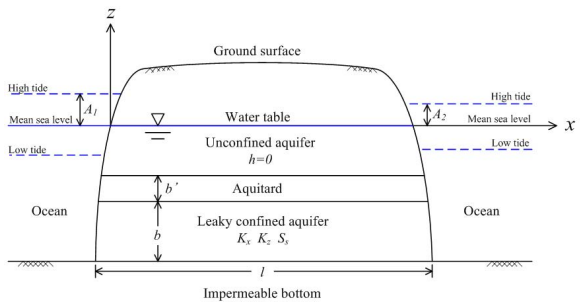

Figure 1. Schematic diagram of a dual-tide coastal leaky aquifer with a finite width.

unconfined aquifer is considered to maintain constant due to its storage effect [*Millham and Howes*, 1995; *Chen and Jiao*, 1999]. Under such a condition the top boundary condition may be expressed as

$$K_z\frac{\partial h}{\partial z}+\frac{K'}{b'}h=0 \quad \text{at} \quad z=0, \tag{5}$$

where K' is hydraulic conductivity of the aquitard.

[15] A simplified equation describing the change of water table for unconfined aquifers without a surface recharge is [*Yeh et al.*, 2010]

$$K_z\frac{\partial h}{\partial z}=-S_y\frac{\partial h}{\partial t} \quad \text{at} \quad z=0, \tag{6}$$

where S_y is specific yield. The equation is applicable to the unconfined aquifer when the ratio of tide amplitude to aquifer thickness is small; that is, the water table variation due to the tide is relatively smaller than the aquifer thickness. If $S_y=0$, the equation reduces to $\partial h/\partial z=0$ describing a no flow boundary for a confined aquifer.

[16] We herein combine equations (5) and (6) for a general top boundary condition as

$$K_z\frac{\partial h}{\partial z}+\frac{K'}{b'}h=-S_y\frac{\partial h}{\partial t} \quad \text{at} \quad z=0, \tag{7}$$

which is applicable to a confined aquifer, an unconfined aquifer, or a leaky confined aquifer. Equation (7) reduces to equation (5) when letting $S_y=0$ for a leaky confined aquifer. On the other hand, equation (7) reduces to equation (6) when setting $K'=0$ for an unconfined aquifer and reduces to $\partial h/\partial z=0$ when setting $K'=0$ and $S_y=0$ for a confined aquifer.

[17] The dimensionless variables for governing equation and boundary conditions are introduced as

$$\begin{aligned} &x_D=\frac{x}{b}, \quad z_D=\frac{z}{b}, \quad t_D=w_1t, \quad h_D=\frac{h}{b}, \quad l_D=\frac{l}{b},\\ &\kappa=\frac{K_z}{K_x}, \quad \omega=\frac{w_2}{w_1}, \quad \varepsilon=\frac{b}{L}, \quad \alpha_1=\frac{A_1}{b}, \quad \alpha_2=\frac{A_2}{b}, \end{aligned} \tag{8}$$

where subscript D represents dimensionless symbol and L is a decay length defined as [*Teo et al.*, 2003]

$$L=\sqrt{\frac{2K_xb}{S_yw_1}} \tag{9}$$

representing the farthest distance that the LHS tide can propagate. Based on these dimensionless variables, equation (1) gives

$$\frac{\partial^2h_D}{\partial x_D}+\kappa\frac{\partial^2h_D}{\partial z_D}=2\sigma\varepsilon^2\frac{\partial h_D}{\partial t_D}, \tag{10}$$

where $\sigma=S_sb/S_y$. Equations (2)–(4) and (7), respectively, become

$$\frac{\partial h_D}{\partial z_D}=0 \quad \text{at} \quad z_D=-1, \tag{11}$$

$$h_D=\alpha_1\cos(t_D) \quad \text{at} \quad x_D=0, \tag{12}$$

$$h_D=\alpha_2\cos(\omega t_D+\phi) \quad \text{at} \quad x_D=l_D, \tag{13}$$

$$\frac{\partial h_D}{\partial z_D}+\beta h_D=\frac{-2\varepsilon^2}{\kappa}\frac{\partial h_D}{\partial t_D} \quad \text{at} \quad z_D=0, \tag{14}$$

where $\beta=K'b/(K_zb')$.

2.2. General Analytical Solution of the Model

[18] Applying direct Fourier method and finite Fourier sine transform to equations (10)–(14) results in

$$\begin{aligned} h_D(x_D,z_D,t_D)=&\alpha_1\,c_1(x_D,z_D)\cos[t_D-\phi_1(x_D,z_D)]\\ &+\alpha_2\,c_2(x_D,z_D)\cos[\omega t_D-\phi_2(x_D,z_D)], \end{aligned} \tag{15}$$

with

$$c_1(x_D,z_D)=\sqrt{\left(\mathrm{Re}\left[h_{xz}(l_D-x_D,z_D,1)\right]\right)^2+\left(\mathrm{Im}\left[h_{xz}(l_D-x_D,z_D,1)\right]\right)^2}, \tag{16}$$

$$c_2(x_D,z_D)=\sqrt{\left(\mathrm{Re}\left[h_{xz}(x_D,z_D,\omega)\right]\right)^2+\left(\mathrm{Im}\left[h_{xz}(x_D,z_D,\omega)\right]\right)^2}, \tag{17}$$

$$\phi_1(x_D,z_D)=\cos^{-1}\left\{\frac{\mathrm{Re}\left[h_{xz}(l_D-x_D,z_D,1)\right]}{c_1(x_D,z_D)}\right\}, \tag{18}$$

$$\phi_2(x_D,z_D)=\cos^{-1}\left\{\frac{\mathrm{Re}\left[h_{xz}(x_D,z_D,\omega)\right]}{c_2(x_D,z_D)}\right\}-\phi, \tag{19}$$

$$\begin{aligned} h_{xz}(x_D,z_D,\omega)=&\frac{\sinh\left[(1+i)\varepsilon\sqrt{\omega\sigma}\,x_D\right]}{\sinh\left[(1+i)\varepsilon\sqrt{\omega\sigma}\,l_D\right]}\\ &+\sum_{n=1}^{\infty}\left\{\frac{-2e^{in\pi}n\pi(\kappa\beta+2i\omega\varepsilon^2)\cosh\left[(1+z_D)\lambda\right]}{(n^2\pi^2+2i\omega l_D^2\sigma\varepsilon^2)[(\kappa\beta-2i\omega\varepsilon^2)\cosh\lambda-\kappa\lambda\sinh\lambda]}\right.,\\ &\left.\times\sin\left(\frac{n\pi x_D}{l_D}\right)\right\} \end{aligned} \tag{20}$$

$$\lambda = \sqrt{\frac{n^2\pi^2}{l_D^2\kappa} + \frac{2i\omega\sigma\varepsilon^2}{\kappa}}, \tag{21}$$

where Re and Im represent the real and imaginary part of the complex expression, respectively; i equals $\sqrt{-1}$; n is an integer from 1, 2, 3, . . . , ∞. For the detailed development of equation (15), readers refer to the Appendix.

2.3. Head Solutions for Leaky Confined Aquifer

[19] If $\varepsilon = 0$ (i.e., $S_y = 0$), equation (20) becomes

$$h_{xz}(x_D, z_D, \omega) = \frac{\sinh[(1+i)\varepsilon' x_D]}{\sinh[(1+i)\varepsilon' l_D]} + \sum_{n=1}^{\infty}\left\{\frac{-2e^{in\pi}n\pi\beta\cosh[(1+z_D)\lambda']}{(n^2\pi^2 + 2i\,l_D^2\varepsilon' 2)(\beta\cosh\lambda' - \lambda'\sinh\lambda')}\sin\left(\frac{n\pi x_D}{l_D}\right)\right\}, \tag{22}$$

with

$$\lambda' = \sqrt{\frac{n^2\pi^2}{l_D^2\kappa} + \frac{2i\varepsilon' 2}{\kappa}}, \qquad \varepsilon' = \frac{b}{L'}, \qquad L' = \sqrt{\frac{2K_x}{S_s w_1 \omega}}. \tag{23}$$

Equation (15) with equations (22) and (23) therefore describes groundwater fluctuations in a leaky confined aquifer. The resulting solution depends on the variable z_D, indicating that the leaky confined aquifer has vertical flow induced from the leakage through the aquitard. The first and second RHS terms of equation (15) describe the head fluctuations due to the LHS and RHS tides, respectively. The coefficients c_1 and ϕ_1 represent attenuation factor and phase lag, respectively, due to the LHS tidal boundary for 2-D groundwater flow. Similarly, the c_2 and ϕ_2 are attenuation factor and phase lag, respectively, due to the RHS tidal boundary.

[20] If $\alpha_2 = 0$ (i.e., $A_2 = 0$), the second term on the RHS of equation (15) vanishes; that is, the leaky confined aquifer is subject to a single tide effect. With $\alpha_2 = 0$ and letting the aquifer width l_D being a large value, equations (15) and (22) then represent the head solution for a tidal leaky confined aquifer extending landward infinitely.

2.4. Head Solution for Unconfined Aquifer

[21] If $\beta = 0$ (i.e., $K' = 0$), equation (20) reduces to

$$h_{xz}(x_D, z_D, \omega) = \frac{\sinh[(1+i)\varepsilon\sqrt{\omega\sigma}x_D]}{\sinh[(1+i)\varepsilon\sqrt{\omega\sigma}l_D]} + \sum_{n=1}^{\infty}\left\{\frac{4in\pi\omega\varepsilon^2 e^{in\pi}\cosh[(1+z_D)\lambda]}{(n^2\pi^2 + 2i\omega l_D^2\sigma\varepsilon^2)(2i\omega\varepsilon^2\cosh\lambda + \kappa\lambda\sinh\lambda)}\sin\left(\frac{n\pi x_D}{l_D}\right)\right\} \tag{24}$$

and thus equation (15) with equation (24) represents a head solution for an unconfined aquifer subject to a dual tide effect.

[22] If $\alpha_2 = 0$ (i.e., $A_2 = 0$) and l_D is very large, equation (15) with equation (24) should give the same results as *Yeh et al.*'s [2010] solution. Under such circumstances, equation (15) becomes the head solution for tidal unconfined aquifers extending landward infinitely.

2.5. Head Solution for Confined Aquifer

[23] If $\varepsilon = 0$, $\beta = 0$, and $\omega = 1$ (i.e., $S_y = 0$, $K' = 0$, and $w_1 = w_2$), equation (20) reduces to

$$h_{xz}(x) = \frac{\sinh\left[(1+i)\,\frac{x}{L''}\right]}{\sinh\left[(1+i)\,\frac{l}{L''}\right]}, \tag{25}$$

where $L'' = \sqrt{2K_x/S_s/w_1}$. In our notation, equation (15) with equation (25) reduces to *Rotzoll et al.*'s [2008] solution which is a head solution in terms of exponential functions for a confined aquifer subject to a dual tide effect. Note that the second term of equation (20) vanishes under these conditions. The solution is then independent of the variable z_D, reflecting the fact that the confined aquifer has no vertical flow.

[24] If $\varepsilon = 0$, $\beta = 0$, $\alpha_2 = 0$, and $l_D \to \infty$ (i.e., $S_y = 0$, $K' = 0$, $A_2 = 0$, and $l \to \infty$), equation (15) further reduces to *Ferris*'s [1951] solution as, in our notation

$$h(x,t) = A_1 e^{-\frac{x}{L''}}\cos\left(w_1 t - \frac{x}{L''}\right), \tag{26}$$

which is indeed the head solution for a tidal confined aquifer extending landward infinitely.

3. Results and Discussion

[25] The default values for dimensional parameters in sections 3.1–3.3 are listed in Table 3. Equation (15) along with equation (24) is used for the case of unconfined aquifers in sections 3.1–3.3. Moreover, equation (15) with equations (22) and (23) is employed for leaky confined aquifers in sections 3.4 and 3.5.

3.1. Comparison With *Yeh et al.*'s [2010] Solution

[26] *Yeh et al.* [2010] presented an analytical solution for describing groundwater fluctuations due to a single tide boundary in an unconfined aquifer extending semi-infinitely. Their solution is in terms of an improper integral to a dummy variable ζ from 0 to ∞ with a complicated integrand containing sine, cosine, exponential functions, infinite series, and indeterminate variables β_0 as well as β_n. Both β_0 and β_n are functions of ζ and should be determined via a root search algorithm. The numerical evaluations therefore involve numerical integration, root-finding algorithm, and accelerated convergence of Shanks' method [*Yang and Yeh*, 2006].

[27] Consider that the aquifer width l is very large and the groundwater is only affected by a neighboring tide. Figure 2 shows the spatial head distributions at $z_D = 0$ (water table) predicted from the present solution and *Yeh et al.*'s [2010] solution for the cases of high tide ($t_D = 2\pi$), mean tide ($t_D = 0.5\pi$; $t_D = 1.5\pi$), and low tide ($t_D = 1.0\pi$). When $K_x = 300$ m day^{-1}, the tide propagation from the LHS tidal boundary reaches the location at $x =$ 500 m. Thus, l is chosen as 1200 m so that the groundwater is affected only by the neighboring tide. The difference

Table 3. The Default Parameter Values

Parameter	Value
K_x (m day^{-1})	300
K_z (m day^{-1})	100
K' (m day^{-1})	0
S_s (m^{-1})	10^{-5}
S_y	0.3
b (m)	50
b' (m)	1
l (m)	500
A_1 (m)	2.5
A_2 (m)	2.5
w_1 (day^{-1})	4π
w_2 (day^{-1})	4π
φ (rad)	0
z (m)	0

between the present solution with $l = 1200$ m and *Yeh et al.*'s [2010] solution is very small, indicating that the present solution can simulate head fluctuations due to a single tidal boundary if l is very large.

3.2. Effect of Specific Yield on Water Table

[28] Unconfined aquifers have gravity drainage when the water table declines, and thus the specific yield affects the amplitude and phase lag of water table fluctuations. Figure 3 demonstrates the spatial distributions of amplitude and phase lag of water table fluctuations for $S_y = 0.1$, 0.2, and 0.3. The aquifer near the coastline, i.e., $x = 0$ or $x = 500$ m has larger amplitude and smaller phase lag than those of the inland aquifer because of the effect of a dual tide. The aquifer with a larger S_y has smaller amplitude and larger phase lag in comparison with that with a smaller one. This is because the aquifer with a large S_y has much gravity drainage when the tide is under the MSL and much capacity of receiving water when the tide is above the MSL. The effect of a tide on groundwater is mainly near the coastline.

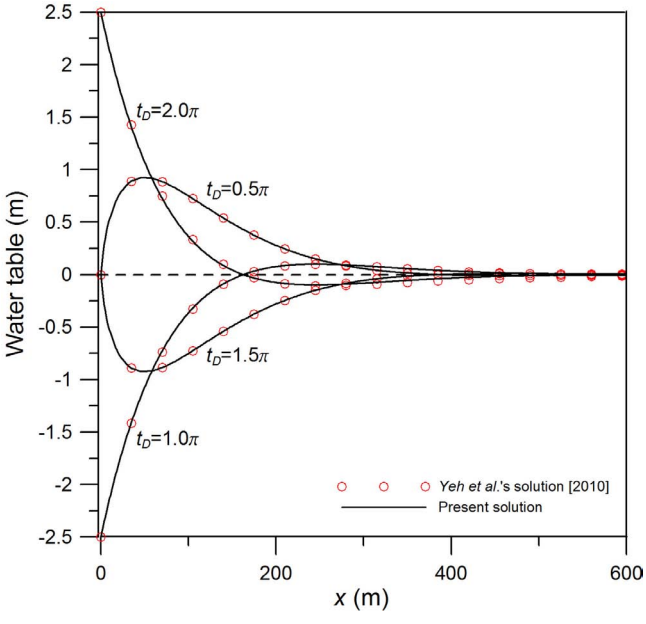

Figure 2. Spatial water table distributions predicted by the present solution and *Yeh et al.*'s [2010] solution.

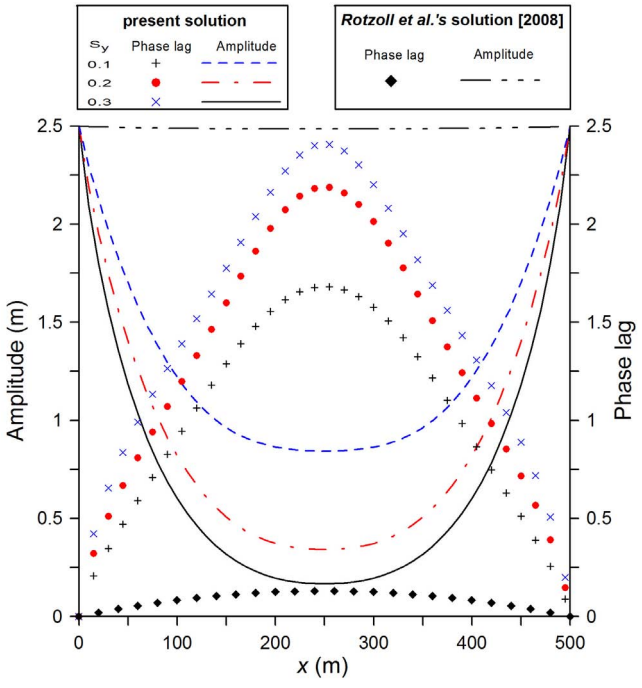

Figure 3. Spatial distributions of amplitude and phase lag of water table fluctuations for various S_y.

[29] The groundwater behaviors of unconfined and confined aquifers in response to a tidal effect are explored through the comparison of the present solution with *Rotzoll et al.*'s [2008] solution as shown in Figure 3. Their solution can be considered as a special case of the present solution when $S_y = 0$; under this circumstance, the free surface equation (equation (6)) reduces to the no flow boundary, $\partial h/\partial z = 0$, for confined aquifers. A confined aquifer has much larger amplitude and smaller phase lag than an unconfined one. The spatial amplitude decreases slightly with distance from the coastline to the inland. In contrast, the spatial phase lag increases slightly with inland distance. Such phenomena indicate that the S_y has significant effects of amplitude attenuation and phase delay on the groundwater fluctuation for an unconfined aquifer. It worth noting that adopting a confined aquifer to approximate an unconfined aquifer results in the overestimate of amplitude and underestimate of phase lag.

3.3. Effect of K_z on Vertical Flow in Unconfined Aquifer

[30] The magnitude of K_z has an effect on the vertical flow in unconfined aquifers. The contour of 2-D groundwater flow and equipotential line (hydraulic head) distributions at various t_D is shown in Figure 4 for $K_z = 30$ m day^{-1} and in Figure 5 for $K_z = 100$ m day^{-1}. The stream function ψ_D can be obtained from Cauchy-Riemann equation as

$$\frac{\partial \psi_D}{\partial x'_D} = -\frac{\partial h_D}{\partial z_D}, \tag{27}$$

where $x'_D = \sqrt{K_z/K_x}\, x_D$ because the aquifer is anisotropic. The function ψ_D can be acquired first by substituting

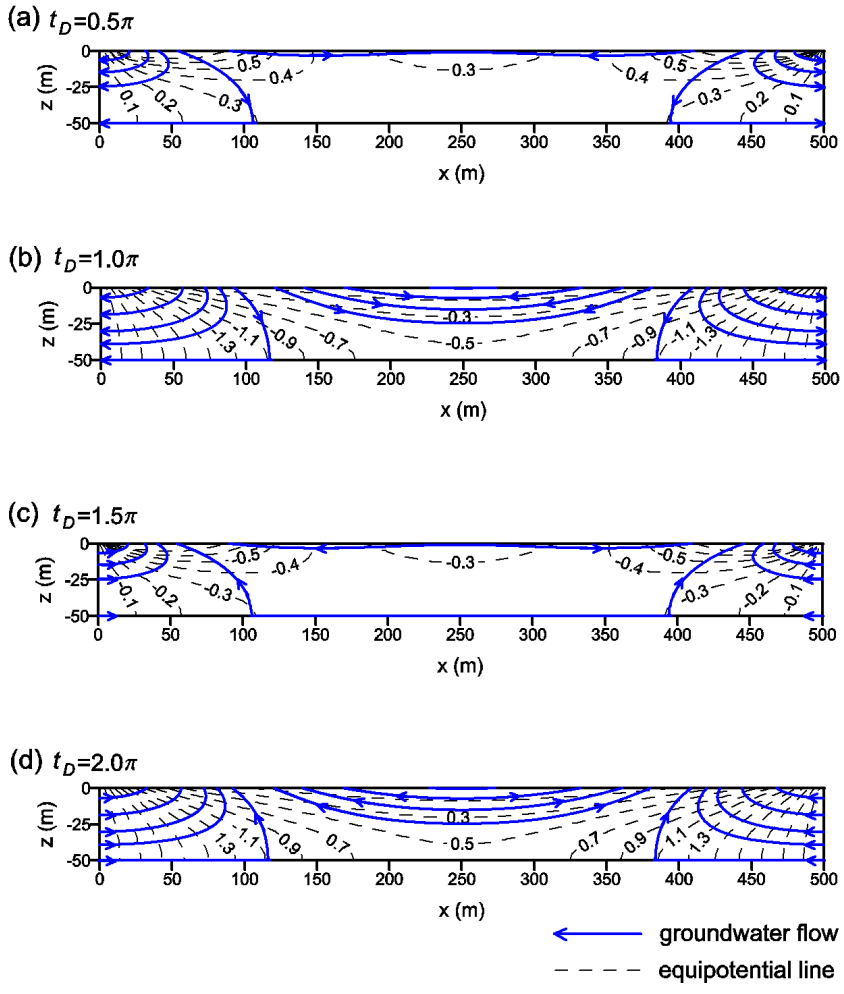

Figure 4. The hydraulic head distributions and flow lines in an unconfined aquifer at various times for $K_x = 300$ and $K_z = 30$ m day^{-1}.

$x_D = \sqrt{K_x/K_z}\,x'_D$ and $l_D = \sqrt{K_x/K_z}\,l'_D$ into equation (15) with equation (24), then by substituting the result into equation (27), and finally by integrating the result with respect to x'_D. The flow line is not perpendicular to the equipotential line because of the aquifer anisotropy. At high tide period, the groundwater near $x = 0$ or 500 m flows landward. The equipotential lines are slanted near $z = 0$, and thus the aquifer near water table has vertical flow. On the other hand, at mean tide ($t_D = 0.5\pi$) period, the equipotential lines are slanted near $x = 0$ and 500 m, and the highest head occurs near $z = 0$ and $x = 40$ m in Figure 4(a) and near $z = 0$ and $x = 60$ m in Figure 5(a). Such a result reflects that the groundwater near coastline has significant vertical flow and flows to the coastline or inland in the slanted direction.

[31] The magnitude of K_z affects the groundwater flow direction near the inland. When at high tide period, the groundwater flows outward in the region between 150 and 350 m for $K_z = 30$ m day^{-1} shown in Figure 4(d). In contrast, the groundwater flows inland in that region for $K_z = 100$ m day^{-1} demonstrated in Figure 5(d). Such a phenomenon reflects that a small K_z produces a slow response of groundwater fluctuations to tide in the inland.

[32] In these two figures, the contours in panels (a) and (b) are identical to those in panels (c) and (d), respectively, except a minus sign before the value. This reflects that the mathematical model is a linear system; that is, the flow line from the ocean to the aquifer is identical to that from the aquifer to the ocean.

3.4. Effects of K'/b' on Vertical Flow in Leaky Confined Aquifer

[33] *Sun et al.* [2008] developed an analytical solution based on 1-D transient groundwater flow equation to describe groundwater fluctuations due to a dual tide in a leaky confined aquifer. Their solution is therefore independent of elevation; that is, the vertical flow induced from the leakage is neglected.

[34] The magnitude of K'/b' affects the vertical flow in a leaky confined aquifer. The contour of 2-D hydraulic head distributions predicted from the present solution and *Sun et al.*'s [2008] solution for various values of K'/b' is demonstrated in Figure 6 at high tide and in Figure 7 at mean tide. Note that the horizontal and vertical hydraulic conductivities of the leaky confined aquifer are 300 and 100 m day^{-1}, respectively. Thus, leakage coefficients K'/b'

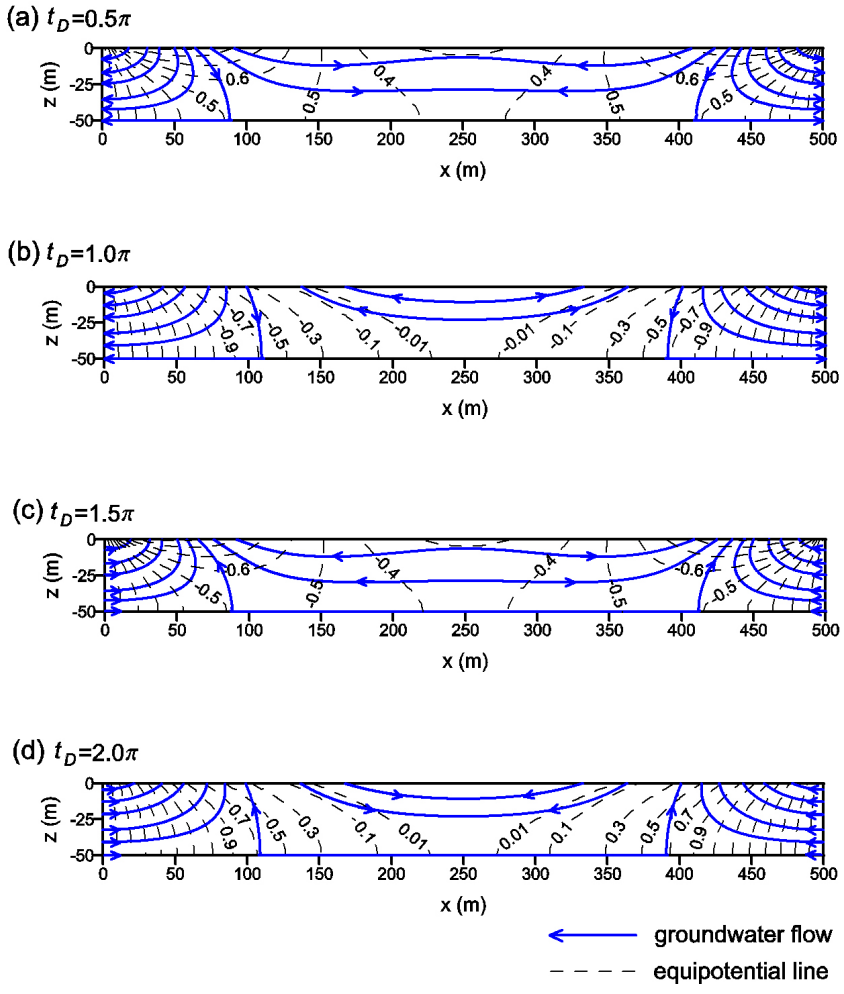

Figure 5. The hydraulic head distributions and flow lines in an unconfined aquifer at various times for $K_x = 300$ and $K_z = 100$ m day^{-1}.

in the range from 10^{-7} to 10^{-1} day^{-1} are regarded as a low permeable medium. For the cases of $K'/b' < 10^{-5}$ day^{-1}, the head contours predicted from the present solution are almost vertical, indicating that the aquifer has no vertical flow. Their solution therefore agrees well with the present solution. However, for the case of $K'/b' = 10^{-3}$ day^{-1}, the head contours from the present solution shown in Figure 6 are slanted in the whole aquifer, especially near the top of the aquifer. This indicates that the leakage produces a large amount of vertical flow even if the upper aquitard is a much lower permeable than the lower aquifer. It is worth noting that their solution agrees well with the present solution for $K'/b' = 10^{-3}$ day^{-1} as illustrated in Figure 7. This indicates that a small amount of leakage occurs at mean tide. For the case of $K'/b' = 10^{-1}$ day^{-1}, the aquifer has abundance of vertical flow, and thus the head from the present solution is much smaller than that from their solution at a specific location. Under such a circumstance, neglecting vertical flow overestimates head.

3.5. Comparison With Observed Data

[35] The geological formation in Garden Island, Australia, was described by *Trefry and Bekele* [2004]. The island is 10 km in length from south to north and 1 to 2 km in width from west to east. The formation of the island consists of the impermeable Mesozoic shale and siltstones below, Safety Bay sand above and Tamala limestone in between. According to *Davidson* [1995], the limestone is sometimes more permeable than the sand. The upper sand is therefore considered as an aquitard, and the lower limestone formation is regarded as a leaky confined aquifer. The average thickness of the aquifer is about 40 m.

[36] In reality, a tide can be considered as the superposition of several harmonic tidal components, and each of them has its own amplitude and period/frequency. The tides and groundwater head in Garden Island are diurnal with dominant K1 and O1 diurnal components. They may be denoted as.

$$h = A_K \times c_K \times \cos(w_K t + \phi_K) + A_O \times c_O \times \cos(w_O t + \phi_O), \tag{28}$$

where A_K, the amplitude of K1 component, is 0.1979 m; c_K, attenuation factor of K1 component, is one; w_K, the frequency of K1 component, is 6.3021 rad/day; ϕ_K, phase lag of K1 component, is zero; A_O, the amplitude of O1

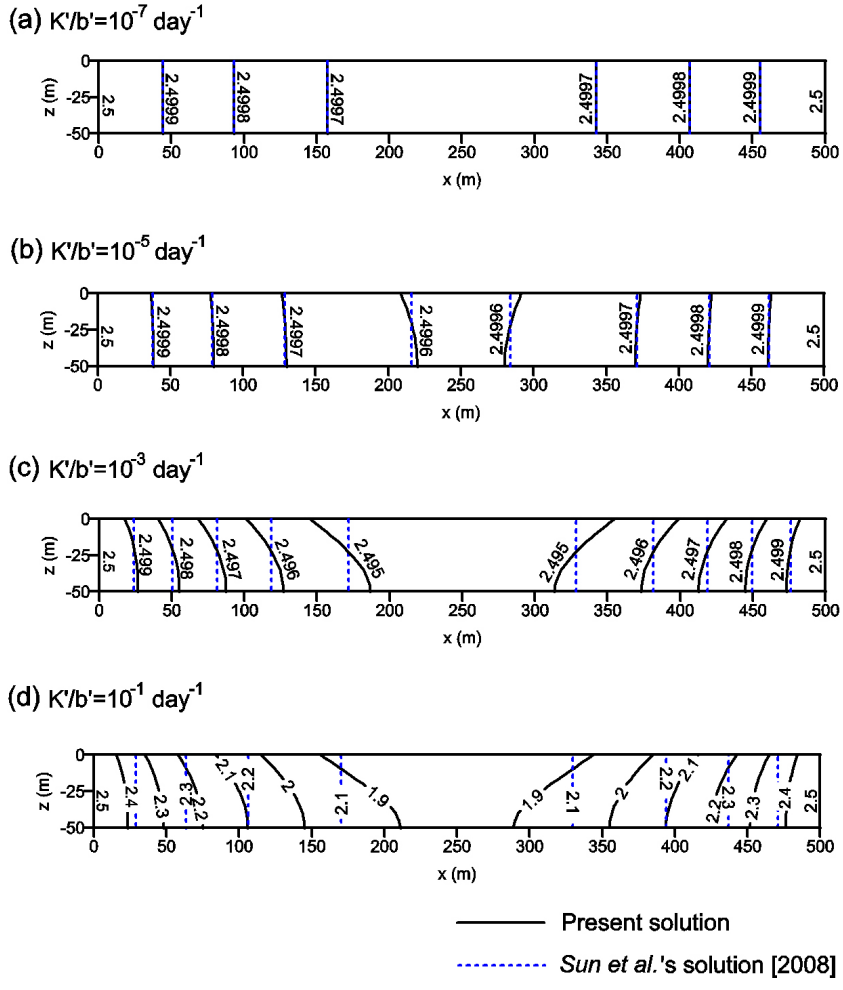

Figure 6. The head distributions predicted by the present solution and *Sun et al.*'s [2008] solution for various K'/b' at high tide.

component, is 0.1065 m; c_O, attenuation factor of O1 component, is one; w_O, the frequency of O1 component, is 5.8432 rad day^{-1}; and ϕ_O, phase lag of O1 component, is zero.

[37] There were 57 day data for head fluctuation measured at eight observation wells in Garden Island. The head fluctuation in each well can be expressed by equation (28) with different c_K and ϕ_K for K1 component and different c_O and ϕ_O for O1 component shown in Table 4 given by *Trefry and Bekele* [2004] obtained by analyzing those head fluctuation data using Fourier spectra analyses.

[38] According to *Freeze and Cherry* [1979], the hydraulic conductivities for limestone and sand may fall in the range of 10^{-4} –1 m day^{-1} and 0.1–1000 m day^{-1}, respectively, and the ratio of the vertical to horizontal hydraulic conductivity range from 10% to 33%. The limestone is more permeable than the sand in Garden Island [*Davidson*, 1995]. Accordingly, the hydraulic conductivities of limestone and sand in Garden Island are chosen as 1 and 0.1 m day^{-1}, respectively, and the ratio of K_z/K_x is chosen as 33%. The other parameter values used to simulate the flow in Garden Island are shown in Table 5.

[39] The values of attenuation factor and phase lag at each observation well can be estimated based on the present solution along with parameters listed in Table 5. The present solution for dimensionless hydraulic head depends on variable z_D since the leakage happens on the upper aquitard. In order to simulate l-D groundwater flow, the hydraulic head, equation (22), is taken as average over the vertical thickness as

$$h_x(x_D,\omega) = \int_{-1}^{0} h_{xz}(x_D,z_D,\omega)\,dz_D = \frac{\sinh\left[(1+i)\varepsilon' x_D\right]}{\sinh\left[(1+i)\varepsilon' l_D\right]} + \sum_{n=1}^{\infty} \frac{-2e^{in\pi}n\pi\beta\sinh\lambda'}{\lambda'(n^2\pi^2+2il_D^2\varepsilon'^2)(\beta\cosh\lambda'-\lambda'\sinh\lambda')}\sin\left(\frac{n\pi x_D}{l_D}\right)\Bigg\}. \tag{29}$$

Substituting $h_{xz} = h_x(x_D,\omega) + h_x(l_D - x_D, 1)$ into equations (16) and (18), respectively, yields the attenuation factor and phase lag as

$$c(x_D) = \sqrt{\{\mathrm{Re}[h_x(x_D,\omega)+h_x(l_D-x_D,1)]\}^2+\{\mathrm{Im}[h_x(x_D,\omega)+h_x(l_D-x_D,1)]\}^2}. \tag{30}$$

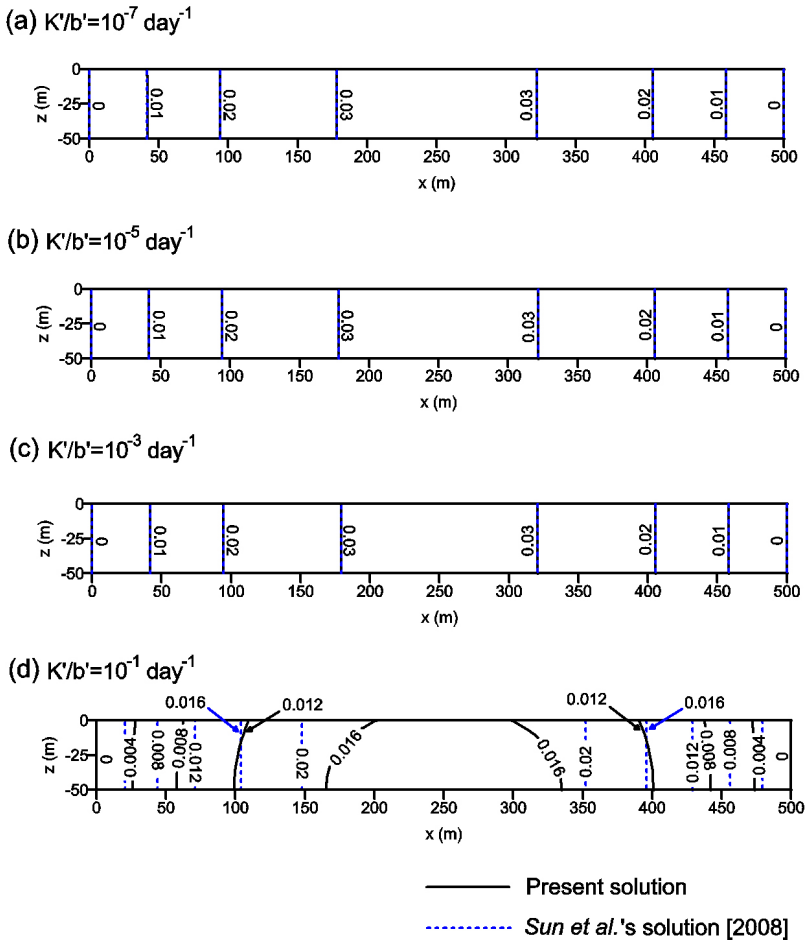

Figure 7. The head distributions predicted by the present solution and *Sun et al.*'s [2008] solution for various K'/b' at mean tide.

$$\phi(x_D) = \cos^{-1}\left\{\frac{\mathrm{Re}\,[h_x(x_D,\omega) + h_x(l_D - x_D, 1)]}{c}\right\}. \quad (31)$$

[40] The attenuation factor and phase lag estimated by equations (30) and (31), respectively, at different observation wells and those estimated from the observed data (Table 5) taken from *Trefry and Bekele* [2004] are shown in Figure 8(a) for K1 component and in Figure 8(b) for O1 component. The results estimated from those two equations have a good agreement with those estimated from fluctuation data observed at all wells except MB8 as indicated in the figure. The MB8 has a larger phase lag than the present result, indicating that groundwater therein has a slow response to a tide effect. Such a discrepancy may be due to the effect of heterogeneity which delays tidal propagation. In other words, there may be a lower permeable medium than limestone occurring between the coastline and MB8.

Table 4. The Well Location and Estimated Tide Components [*Trefry and Bekele*, 2004]

		K1 Component		O1 Component	
Well	x (m)	Attenuation Factor	Phase Lag	Attenuation Factor	Phase Lag
West coast	0	1	0	1	0
MB6	264	0.119	0.120	0.059	0.219
MB8	267	0.108	0.283	0.113	0.272
MB7	304	0.069	0.199	0.074	0.186
MB11	481	0.014	0.325	0.008	0.297
MB5	601	0.007	0.407	0.003	0.375
MB3	788	0.024	0.238	0.025	0.232
MB2	849	0.040	0.229	0.040	0.192
MB1	961	0.094	0.135	0.103	0.126
East coast	1380	1	0	1	0

Table 5. The Hydraulic Parameters and Aquifer Data in Garden Island, Australia

Parameter	Value
K_x (m day^{-1})	1
K_z (m day^{-1})	$0.33K_x$
K' (m day^{-1})	0.1
b (m)	40
S_s (m^{-1})	$10^{-3}/b$
S_y	0
b' (m)	1
l (m)	1380
w_1 for K1 component (rad day^{-1})	6.3021
w_1 for O1 component (rad day^{-1})	5.8432
w_2 (rad day^{-1})	w_1

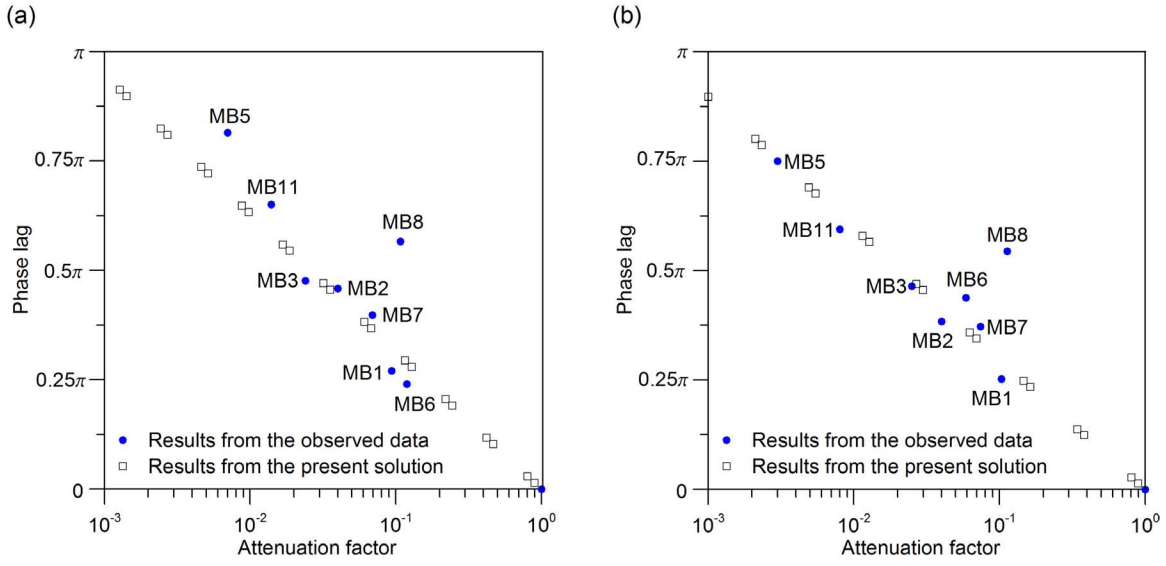

Figure 8. The attenuation factor and phase lag estimated from the present solution and those estimated from the head fluctuation data observed at Garden Island reported by *Trefry and Bekele* [2004] for (a) K1 component and (b) O1 component.

4. Concluding Remarks

[41] A mathematical model is developed for describing groundwater fluctuations due to a dual tide effect in island aquifers. The top boundary of the aquifer is considered to combine the free surface equation describing the change of water table and equation describing the aquitard leakage rate. The solution of the model is derived by direct Fourier method, finite Fourier sine transform, and contour integral. The solution can be used for describing head distributions in an unconfined aquifer if setting $K' = 0$, leaky confined aquifer if $S_y = 0$, and confined aquifer if $K' = 0$ and $S_y = 0$. The attenuation factor and phase lag evaluated from the present solution agrees reasonably well with those estimated from the observed data reported by *Trefry and Bekele* [2004]. Some behaviors of groundwater flow due to a dual tide effect for an unconfined aquifer and leaky confined aquifer are investigated, and the conclusions are made below:

[42] 1. The present solution expressed in a closed form gives the same head prediction as *Yeh et al.*'s [2010] solution when the aquifer width is very large. Obviously, the present solution can be used to describe groundwater fluctuations due to a single tide effect in aquifers extending semi-infinitely.

[43] 2. Specific yield has a significant effect on groundwater fluctuations in an unconfined aquifer. The aquifer with larger specific yield has a smaller amplitude and larger phase lag of water table fluctuations.

[44] 3. A large quantity of vertical flow is produced around water table near coastlines in an unconfined aquifer.

[45] 4. A vertical hydraulic conductivity produces a significant effect on directions of groundwater flow in an unconfined aquifer. At high tide or low tide, a small vertical hydraulic conductivity produces opposite directions of groundwater flow in the inland to that near coastline.

[46] 5. A leaky confined aquifer may have significant vertical flow even if the upper aquitard is more impermeable than the lower leaky confined aquifer. The present solution can be adopted to describe the flow in such an aquifer.

[47] 6. The model without considering vertical flow in a leaky confined aquifer or an unconfined aquifer overestimates hydraulic head.

Appendix A: The Derivation of Equation (15)

[48] The mathematical model is a linear system containing equations (1)–(7). The model with a dual tide boundary is therefore expressed as the sum of two models with a single-side tide boundary based on the principle of superposition. For each of these two models, the boundary condition on the other side of the island is considered as $h_D = 0$.

[49] Based on the direct Fourier method, the solution of the model with only one tidal boundary can be expressed as

$$h_{D2}(x_D, z_D, t_D) = \mathrm{Re}\left[\alpha_2 \cdot h_{xz}(x_D, z_D, \omega) \cdot e^{i(\omega t_D + \phi)}\right]. \tag{A1}$$

Substituting equation (A1) into the boundary condition $h_D = 0$ at $x_D = 0$ and equations (10) and (11) as well as (13) and (14) and then eliminating exponential term involved in time yield a second-order partial differential equation (PDE) and four boundary conditions in term of h_{xz}. Applying finite Fourier sine transform to the PDE and associated boundary conditions leads to a second-order ordinary differential equation (ODE) and two boundary conditions to the variable z_D as

$$\kappa \frac{\partial^2 \overline{h_{xz}}}{\partial z_D} - \left(\frac{n^2\pi^2}{l_D} + 2i\sigma\omega\varepsilon^2\right)\overline{h_{xz}} = -\frac{n\pi}{l_D}(-1)^{n+1}, \tag{A2}$$

with

$$\frac{\partial \overline{h_{xz}}}{\partial z_D} = 0 \quad \text{at} \quad z = -1, \tag{A3}$$

$$\frac{\partial \overline{h_{xz}}}{\partial z_D} + \beta \overline{h_{xz}} = -\frac{2i\omega\varepsilon^2}{\kappa}\overline{h_{xz}} \quad \text{at} \quad z = 0. \tag{A4}$$

Solving the ODE yields the solution in Fourier sine domain. Inverting this solution by directly using formula results in

$$h_{xz}(x_D, z_D, \omega) = \sum_{n=-\infty}^{\infty}\left[-\frac{(-1)^n n\pi}{n^2\pi^2 + 2i\sigma\omega l_D^2\varepsilon^2}\sin\left(\frac{n\pi x_D}{l_D}\right)\right] + \sum_{n=1}^{\infty}\left[\frac{2e^{in\pi}n\pi(\kappa\beta - 2i\omega\varepsilon^2)\cosh[(1+z_D)\lambda]}{(n^2\pi^2 + 2i\omega l_D^2\sigma\varepsilon^2)[(\kappa\beta - 2i\omega\varepsilon^2)\cosh\lambda - \kappa\lambda\sinh\lambda]} \times \sin\left(\frac{n\pi x_D}{l_D}\right)\right]. \tag{A5}$$

[50] The first term on the RHS of equation (A5) is an oscillating series which can further reduce to a closed-form result without series by contour integral and residue theorem. Consider an integral as

$$I = \oint_{Ca} \frac{f(z)}{\sin(\pi z)}dz, \tag{A6}$$

where z is a variable in the complex plan; c_a is a closed path consisting of two straight lines parallel to the real axis and two semicircles with a radius r as illustrated in Figure A1(a); and $f(z)$ is an arbitrary single value function without the poles occurring at the real axis. The integrand $f(z)/\sin(\pi z)$ has simple poles occurring at $z = 0, \pm1, \pm2, \pm3 \ldots$ derived from $\sin(\pi z) = 0$. The residue for each pole inside the closed path can be written as $2if(z)/\cos(\pi z)$ by the residue theorem. The sum of the residue for each pole is the integral result of equation (A6) as

$$I = 2i\sum_{z=-\infty}^{\infty}\frac{f(z)}{\cos(\pi z)} = 2i\sum_{n=-\infty}^{\infty}(-1)^n f(n). \tag{A7}$$

Note that equation (A7) has the form of oscillating series corresponding to the first term on the RHS of equation (A5) if $f(n) = -n\pi\sin(n\pi x_D/l_D)/(n^2\pi^2 + 2i\sigma\omega l_D^2\varepsilon^2)$. The sum of this oscillating series is therefore equal to the integral result of equation (A6).

[51] The result of the integral in equation (A6) for the closed path c_a in Figure A1(a) is equal to that for another closed path c_b in Figure A1(b). The path c_b consists of two straight lines parallel to the real axis, a small semicircle with radius r as well as a large circle with radius R. The integrals along the semicircle when $r \to 0$ and the circle when $R \to \infty$ are both zero. The path c_b is therefore regarded as closed path c_a if $r \to 0$ and $R \to \infty$. The poles at $z = n = 0, \pm1, \pm2, \pm3 \ldots$ are outside the path c_b. In contrast, the two simple poles derived from letting the denominator of $f(n)$ to be zero are inside the path c_b. By the residue theorem, the integral result of equation (A6) is the sum of the residues for these two poles. The sum of the oscillating series therefore reduces to a closed-form result which is indeed the first term on the RHS of equation (20).

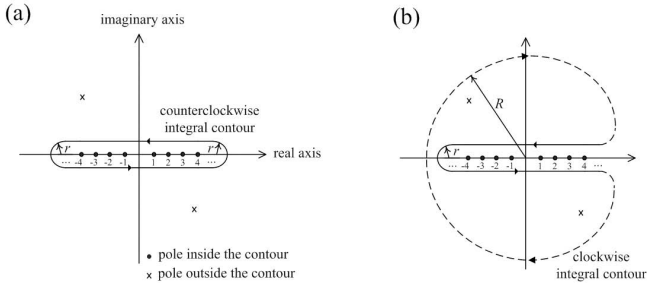

Figure A1. Contour of integral path in the complex plan.

[52] The solution of the model with a single tidal boundary on the other side can be directly obtained by replacing α_2, x_D, ω, and ϕ with α_1, l_D-x_D, 1, and 0, respectively, to equation (A1). The result is then expressed as

$$h_{D1}(x_D, z_D, t_D) = \mathrm{Re}\left[\alpha_1 \cdot h_{xz}(l_D - x_D, z_D, 1)\cdot e^{it_D}\right]. \tag{A8}$$

[53] The sum of equations (A1) and (A8) yields the solution for the dual-tide boundary based on the principle of superposition. The result can further reduce to equation (15) based on the relationships $e^{it_D} = \cos(t_D) + i\sin(t_D)$ and $e^{i(\omega t_D + \phi)} = \cos(\omega t_D + \phi) + i\sin(\omega t_D + \phi)$.

[54] **Acknowledgments.** This study was partly supported by the Taiwan National Science Council under grants NSC 99-2221-E-009-062-MY3, NSC 100-2221-E-009-106, and NSC101-3113-E-007-008. The authors would like to thank three anonymous reviewers for their valuable and constructive comments that helped improve the clarity of our presentation.

References

Balugani, E., and M. Antonellini (2011), Barometric pressure influence on water table fluctuations in coastal aquifers of partially enclosed seas: An example from the Adriatic coast, Italy, *J. Hydrol*, *400*(1–2), 176–186, doi:10.1016/j.jhydrol.2011.01.040.

Bokuniewicz, H., and B. Pavlik (1990), Groundwater seepage along a Barrier Island, *Biogeochemistry*, *10*(3), 257–276.

Chang, Y. C., D. S. Jeng, and H. D. Yeh (2010), Tidal propagation in an oceanic island with sloping beaches, *Hydrol. Earth Syst. Sci.*, *14*(7), 1341–1351, doi:10.5194/hess-14-1341-2010.

Chen, C. X., and J. J. Jiao (1999), Numerical simulation of pumping tests in multilayer wells with non-Darcian flow in the wellbore, *Ground Water*, *37*(3), 465–474.

Chuang, M. H., and H. D. Yeh (2007), An analytical solution for the head distribution in a tidal leaky confined aquifer extending an infinite distance under the sea, *Adv. Water Resour*, *30*(3), 439–445, doi:10.1016/j.advwatres.2006.05.011.

Chuang, M. H., and H. D. Yeh (2008), An analytical solution for tidal propagation in a leaky aquifer extending finite distance under the sea, *J. Hydraul. Eng.*, *134*(4), 447–454, doi:10.1061/(ASCE)0733-9429(2008)134:4(447).

Chuang, M. H., and H. D. Yeh (2011), A generalized solution for groundwater fluctuation in a tidal leaky aquifer system, *J. Earth Syst. Sci.*, *120*(6), 1055–1066, doi:10.1007/s12040-011-0128-8.

Chuang, M. H., C. S. Huang, G. H. Li, and H. D. Yeh (2010), Groundwater fluctuations in heterogeneous coastal leaky aquifer systems, *Hydrol. Earth Syst. Sci.*, *14*(10), 1819–1826, doi:10.5194/hess-14-1819-2010.

Chuang, M. H., M. Asadi, A., and H. D. Yeh (2012), A perturbation solution for head fluctuations in a coastal leaky aquifer system considering water table over-height, *Hydrolog. Sci. J.*, *57*(1), 162–172, doi:10.1080/02626667.2011.637496.

Davidson, W. A. (1995), Hydrogeology and groundwater resources of the Perth Region, Western Australia, *West. Aust. Geol. Surv. Bull.*, *142*, 49–60.

Ferris, J. G. (1951), Cyclic fluctuations of water level as a basis for determining aquifer transmissibility, *Int. Assoc. Hydrolog. Sci.*, *33*(2), 148–155.

Freeze, R. A., and J. A. Cherry (1979), *Groundwater*, 604 pp., Prentice-Hall, Englewood Cliffs, NJ.

Geng, X., H. Li, M. C. Boufadel, and S. Liu (2009), Tide-induced head fluctuations in a coastal aquifer: Effects of the elastic storage and leakage of the submarine outlet-capping, *Hydrogeol. J.*, *17*(5), 1289–1296, doi:10.1007/s10040-009-0439-x.

Guo, H., J. J. Jiao, and H. Li (2010), Groundwater response to tidal fluctuation in a two-zone aquifer, *J. Hydrol.*, *381*(3–4), 364–371, doi:10.1016/j.jhydrol.2009.12.009.

Guo, Q., H. Li, M. C. Boufadel, Y. Xia, and G. Li (2007), Tide-induced groundwater head fluctuation in coastal multi-layered aquifer systems with a submarine outlet-capping, *Adv. Water Resour.*, *30*(8), 1746–1755, doi:10.1016/j.adwatres.2007.01.003.

Jeng, D. S., L. Li, and D. A. Barry (2002), Analytical solution for tidal propagation in a coupled semi-confined/phreatic coastal aquifer, *Adv. Water Resour.*, *25*(5), 577–584, doi:10.1016/S0309-1708(02)00016-7.

Jiao, J. J., and Z. Tang (1999), An analytical solution of groundwater response to tidal fluctuation in a leaky confined aquifer, *Water Resour. Res.*, *35*(3), 747–751.

Kacimov, A., and O. Abdalla (2010), Water table response to a tidal agitation in a coastal aquifer: The Meyer-Polubarinova-Kochina theory revisited, *J. Hydrol.*, *392*(1–2), 96–104, doi:10.1016/j.jhydrol.2010.07.040.

Li, G., and C. Chen (1991), Determining the length of confined aquifer roof extending under the sea by the tidal method, *J. Hydrol.*, *123*(1–2), 97–104.

Li, G., H. Li, and M. C. Boufadel (2008), The enhancing effect of the elastic storage of the seabed aquitard on the tide-induced groundwater head fluctuation in confined submarine aquifer systems, *J. Hydrol.*, *350*(1–2), 83–92, doi:10.1016/j.jhydrol.2007.11.037.

Li, H., and J. J. Jiao (2001), Tide-induced groundwater fluctuation in a coastal leaky confined aquifer system extending under the sea, *Water Resour. Res.*, *37*(5), 1165–1171.

Li, H., G. Li, J. Cheng, and M. C. Boufadel (2007), Tide-induced head fluctuations in a confined aquifer with sediment covering its outlet at the sea floor, *Water Resour. Res.*, *43*(3), W03404, doi:10.1029/2005WR004724.

Li, L., D. A. Barry, F. Stagnitti, J. Y. Parlange, and D. S. Jeng (2000), Beach water table fluctuations due to spring-neap tides: Moving boundary effects, *Adv. Water Resour.*, *23*(8), 817–824, doi:10.1016/S0309-1708(00)00017-8.

Millham, N. P., and B. L. Howes (1995), A comparison of methods to determine K in a shallow coastal aquifer, *Ground Water*, *33*(1), 49–57.

Rotzoll, K., A. I. EI-Kadi, and S. B. Gingerich (2007), Estimating hydraulic properties of volcanic aquifers using constant rate and variable-rate aquifer tests, *J. Am. Water Resour. Assoc.*, *43*(2), 334–345, doi:10.1111/j.1752-1688.2007.00026.x.

Rotzoll, K., A. I. EI-Kadi, and S. B. Gingerich (2008), Analysis of an unconfined aquifer subject to asynchronous dual-tide propagation, *Ground Water*, *46*(2), 239–250, doi:10.1111/j.1745-6584.2007.00412.x.

Song, Z., L. Li, J. Kong, and H. Zhang (2007), A new analytical solution of tidal water table fluctuations in a coastal unconfined aquifer, *J. Hydrol.*, *340*(3–4), 256–260, doi:10.1016/j.jhydrol.2007.04.015.

Sun, P., H. Li, M. C. Boufadel, X. Geng, and S. Chen (2008), An analytical solution and case study of groundwater head response to dual tide in an island leaky confined aquifer, *Water Resour. Res.*, *44*(12), W12501, doi:10.1029/2008WR006893.

Teo, H. T., D. S. Jeng, B. R. Seymour, D. A. Barry, and L. Li (2003), A new analytical solution for water table fluctuations in coastal aquifers with sloping beaches, *Adv. Water Resour.*, *26*(12), 1239–1247, doi:10.1016/j.advwatres.2003.08.004.

Teo, H. T., D. S. Jeng, B. R. Seymour, D. A. Barry, and L. Li (2006), Two-dimensional analytical solution for tide-induced water table fluctuations in a sandy rhythmic coastline, *J. Coastal Res.*, *3*(39), 1665–1670.

Trefry, M. G. and E. Bekele (2004), Structural characterization of an island aquifer via tidal methods, *Water Resour. Res.*, *40*(1), W01505, doi:10.1029/2003WR002003.

Van Der Kamp, G. (1972), Tidal fluctuations in a confined aquifer extending under the sea, *24th International Geological Conference*, Montreal, Quebec, Canada, 11, 101–106.

Xia, Y., H. Li, M. C. Boufadel, Q. Guo, and G. Li (2007), Tidal wave propagation in a coastal aquifer: Effects of leakages through its submarine outlet-capping and offshore roof, *J. Hydrol.*, *337*(3–4), 249–257, doi:10.1016/j.jhydrol.2007.01.036.

Yang, S. Y., and H. D. Yeh (2006), A novel analytical solution for constant-head test in a patchy aquifer, *Int. J. Numer. Anal. Met.*, *30*(12), 1213–1230, doi:10.1002/nag.523.

Yeh, H. D., C. S. Huang, Y. C. Chang and D. S. Jeng (2010), An analytical solution for tidal fluctuations in unconfined aquifers with a vertical beach, *Water Resour. Res.*, *46*, W10535, doi:10.1029/2009WR008746.

C.-H. Chang, C.-S. Huang, and H.-D. Yeh, Institute of Environmental Engineering, National Chiao Tung University, 1001 University Rd., Hsinchu 30010, Taiwan. (hdyeh@mail.nctu.edu.tw)